# D–$^3$He proton spectra for diagnosing shell $\rho R$ and fuel $T_i$ of imploded capsules at OMEGA

C. K. Li, D. G. Hicks, F. H. Séguin, J. A. Frenje, and R. D. Petrasso[a)]
*Plasma Science and Fusion Center, Massachusetts Institute of Technology, Cambridge, Massachusetts 02139*

J. M. Soures, P. B. Radha, V. Yu. Glebov, C. Stoeckl, D. R. Harding, J. P. Knauer, R. Kremens,[b)] F. J. Marshall, D. D. Meyerhofer, S. Skupsky, S. Roberts, and C. Sorce
*Laboratory for Laser Energetics, University of Rochester, Rochester, New York 16423*

T. C. Sangster, T. W. Phillips, and M. D. Cable[c)]
*Lawrence Livermore National Laboratory, Livermore, California 94550*

R. J. Leeper
*Sandia National Laboratories, Albuquerque, New Mexico 87185*

(Received 15 November 1999; accepted 17 February 2000)

Recent work has resulted in the first high-resolution, spectroscopic measurements of energetic charged particles on OMEGA laser facility [T. R. Boehly *et al.*, Opt. Commun. **133**, 496 (1997)]. Energy spectra of charged fusion products have been obtained from two spectrometers, and have been used to deduce various physical quantities in imploded capsules. In this paper the first use of 14.7 MeV deuterium–helium3 (D–$^3$He) proton spectra for diagnosing shell areal density ($\rho R$) and fuel ion temperature ($T_i$) is discussed. For thick-plastic shell capsules, shell areal densities between 20 and 70 mg/cm$^2$ and ion temperatures between 3 and 5 keV have been determined. The spectral linewidths associated with such capsules are found to be wider than the doppler widths. This effect, the focus of future study, is the result of $\rho R$ evolution during the burn; or is the result of an extended burn region; or results from nonuniformities in the shell. For thin-glass shell capsules, the spectral linewidths are dominated by the doppler width, and ion temperatures between 10 and 15 keV were determined. These measurements have been also compared and contrasted with the results from neutron measurements and from one-dimension hydrodynamic simulations. © *2000 American Institute of Physics.* [S1070-664X(00)01306-9]

## I. INTRODUCTION

Attaining high gain in inertial confinement fusion (ICF) experiments requires sufficient capsule compression to achieve high density and temperature. For the hot spot implosion scenario, for example, the capsule is envisioned to be compressed so as to form two different regions, a small mass, lower density fuel at the center with high temperature (~10 keV), and a larger mass of high density, low temperature fuel surrounding the hot spot. One way currently planned to achieve this objective is to, first, cryogenically cool a capsule, so that the fuel will initially form a solid layer, and then to adiabatically compress it.[1,2] In order to explore the physics of high-compression implosions, and as a means to develop energetic charged particles as a diagnostic, a series of spherical implosions were conducted on OMEGA laser facility at University of Rochester[3] to implode gas-filled deuterium–helium3 (D–$^3$He) plastic capsules. To investigate the conditions achieved by these implosions, we utilize, in large part, the 14.7 MeV protons generated from D–$^3$He fusion.

For the range of plastic-shell thickness 10–25 $\mu$m capsule radii ~450–480 $\mu$m and gas fills from 3–15 atms, capsule shell areal densities ($\rho R$) of 20–70 mg/cm$^2$ are achieved. For such areal densities, the 14.7 MeV D–$^3$He proton is an ideal probe since it can easily escape from the capsule, yet undergoes sufficient slowing that its energy loss can be accurately measured. Earlier work on charged-particle diagnostics for ICF capsules were either very low-resolution spectroscopic studies based on range filters[4,5] or focused on low-energy charged particles [such as deuterium–deuterium (D–D) protons[6] and (deuterium–tritium) D–T alphas[7]], which cannot escape from the thick-shell capsules discussed herein.

As we will show, two important physical quantities are deduced by the spectroscopic measurements of the 14.7 MeV protons: shell areal densities and plasma ion temperature ($T_i$). As 14.7 MeV protons travel through the capsule, the protons lose energy in direct proportion to the areal density. Because the fuel has a relatively high temperature and small $\rho R$, most of the energy loss occurs in the low temperature high density shell, for which $\rho R$ is largely temperature insensitive. In addition, since the proton yield and spectrum are temperature sensitive, ion temperatures can be deduced in two ways. The first is the ''ratio method,'' which utilizes the ratio of the D–$^3$He proton yield to either the D–D proton yield or the D–D neutron yield (the ratio of the reaction rates

[a)]Also Visiting Senior Scientist at Laboratory for Laser Energetics.
[b)]Presently at Questra Consulting.
[c)]Presently at Xenogen.

 

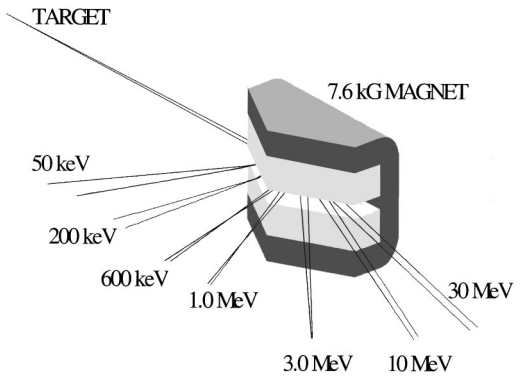


FIG. 1. Schematic diagram illustrating the concept of the charged-particle spectrometer and showing sample proton trajectories. A 7.6 kG pentagonal dipole magnet, 28 cm in its longest dimension, disperses protons in the range 0.1–40 MeV according to the ratio of momentum to charge. A curvilinear array of CR-39 nuclear track detectors is placed around the edge of the magnet and normal to the dispersed beam. The large dynamic range of these detectors allows measurement of fusion yields from $10^7$–$10^{16}$.

for D–$^3$He and D–D is very temperature sensitive for $T_i \leqslant 25$ keV). The second technique is the ''doppler method,'' which utilizes the measured spectral width of the D–$^3$He protons. However, as will be shown, this method is only valid for thin-glass-shell capsules for which the proton spectral width is dominated by the doppler width.

This paper presents, for the first time, high-resolution 14.7 MeV proton spectra generated from ICF experiments, and discusses their utility for measuring shell areal densities and plasma ion temperatures of the imploded capsules. In addition, a result of particular interest is the finding that the (down-shifted) 14.7 MeV linewidth, for thick-plastic-shell implosions, is larger than the doppler width. We anticipate that this effect is related to fundamental aspects of the implosion dynamics, possibly due to $\rho R$ evolution during the burn, or to the presence of an extended burn region, or the result of shell nonuniformities. In Sec. II, the two charged-particle spectrometers (CPS-1 and CPS-2) are described. The experimental conditions and nature and characteristics of the basic data are presented in Sec. III. The determination of shell $\rho R$ and fuel $T_i$ is described in Sec. IV. Section V summarizes the main results.

## II. THE CHARGED-PARTICLE SPECTROMETERS ON OMEGA

Two newly developed charged-particle spectrometers (CPS-1 and CPS-2) have been implemented on OMEGA for delineating and characterizing capsule implosions through charged particles, both nuclear lines and continua. The spectrometers are nearly identical, and each utilizes a 7.6 kG permanent magnet[8,9] constructed of a neodymium–iron–boron alloy with a steel yoke, as shown in Fig. 1. Incoming particles are collimated by a slit whose width can be varied between 1 and 10 mm (giving solid angles between $10^{-6}$ and $10^{-5}$), as appropriate for expected flux levels. The magnet separates particles into different trajectories according to the ratio of momentum to charge. Nearly contiguous pieces of CR39 are used as particle detectors, and are positioned throughout the dispersed beam but normal to the particle flux. Both the energy and the species of the particle generating a track in CR39 can be determined through the combined knowledge of its trajectory (determined by its position on the CR39) and the track diameter. This configuration allows about 85% coverage over the proton energy range from 0.1 MeV to 40 MeV (there are small gaps in coverage between separate pieces of CR39). An earlier instrument using this basic technique (coupling a charged-particle spectrometer to a CR39 particle detector) is described in Ref. 10.

The dynamic range of the two spectrometers for fusion yields extends from about $10^7$ up to $10^{16}$.[11] The energy resolution[12] varies with energy, being about 30 keV at 2 MeV and about 50–100 keV at 15 MeV. (All spectra, including that from the 14.7 MeV proton, are an integral over the burn duration.) The two spectrometers are 101° apart, thereby enabling studies of implosion symmetry to be undertaken. CPS-2 (CPS-1) is placed inside (outside) the OMEGA chamber at 100 cm (235 cm) from the target (the wall chamber radius is at 165 cm).

## III. THE EXPERIMENTS AND THE NATURE OF THE SPECTRAL DATA

In order to lay the framework for the detailed studies of Sec. IV, we discuss here the nature of the spectral data and some general features of how the data can be used. We start with a general discussion of the overall experiment.

### A. Experiments

The experiments were conducted on OMEGA with 60 beams of frequency-tripled (0.35 $\mu$m) UV light smoothed by Spectral Dispersion (2D–SSD with 0.2 THz bandwidth).[13] The laser pulses were 1 ns square (on top). Laser energy ranged from 25 to 29 kJ, with intensity $\sim 1\times 10^{15}$ W/cm$^2$ and spot size $\sim$1 mm on target. Typical rms variation of the UV energy incident on target was between 5–10 %. D–D neutron yields were measured using neutron time-of-flight detectors (TOF).[14–16] Using the MEDUSA single-hit neutron detector array[17,18] or other neutron diagnostics, an upper limit on the compressed fuel $\rho R$ was determined by secondary D–T neutrons. Fusion burn history was obtained using the neutron temporal detector (NTD),[19] and typical fusion burn durations were $\sim$150–200 ps, with the bang time occurring at different times relative to the laser pulse.

### B. D–$^3$He proton spectra

Implosions of both thin-glass- (usually $\leqslant 3$ $\mu$m) and thick-plastic- (usually 10–25 $\mu$m) shell capsules have been used in this study. These capsules were filled to the ratio of 1 molar of $D_2$ and 2 molar of $^3$He. Total capsule pressures ranged from 3 to 15 atms. Thin-glass-shell capsules are of interest as they result in high temperatures and therefore high yields. There is also little spectral distortion associated with these implosions since, among other reasons, ranging effects are insignificant for 14.7 MeV protons. The thick-plastic-shell capsules, which are more ICF relevant, lead to significant ranging and energy loss of the protons and, as we will

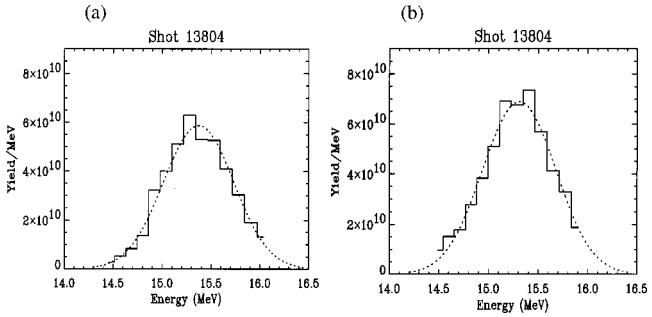


FIG. 2. (a) D–$^3$He proton spectrum measured using CPS-2 with 1 mm slit for shot 13804. This is a D–$^3$He shot with 3.3 $\mu$m glass shell. (b) D–$^3$He proton spectrum measured using CPS-1 with 1 mm slit for the same shot. Similar energy up-shifts (about 0.6 MeV) were observed for both spectrometers (absolute energy uncertainty is about 50–100 keV).

discuss, there is also the intriguing feature that the (down-shifted) 14.7 MeV spectral linewidth is broader than the doppler width.

Typical proton spectra from thin-glass-shell capsule implosions are illustrated in Figs. 2(a) and 2(b) for shot 13804, measured by CPS-2 and CPS-1, respectively. This was a D–$^3$He target with 3.3 $\mu$m glass shell. Both spectra are well approximated by a Gaussian distribution, and both have similar yields to within about 15% (Ref. 20) and energy up-shifts (about 0.6 MeV due to the particle accelerations to be discussed). Random variations of energy measurements between CPS-1 and CPS-2 are usually negligible.[21] Little, if any, energy loss occurs in these thin-glass-shell capsules. In contrast, Fig. 3 depicts a high-resolution spectrum from a thicker-plastic-shell capsule (14.5 $\mu$m CH) implosion measured by CPS-2 (also with 1 mm slit). The spectrum is down-shifted by ~0.8 MeV from 14.7 MeV, which is a clear indication of significant areal density (we discuss later why accelerations or up-shifts are probably negligible for such implosions). In addition, the profile is both slightly non-Gaussian and wider than the doppler width, an indication that, for example, the shell $\rho R$ is evolving during the burn

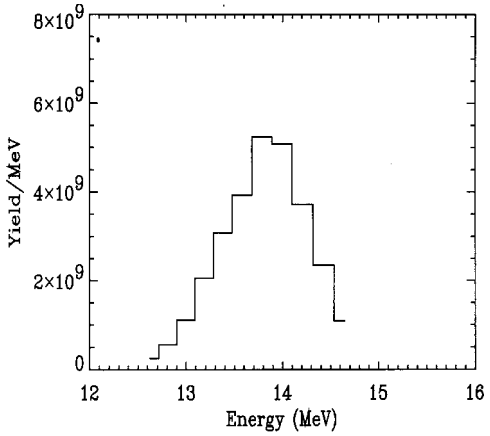


FIG. 3. D–$^3$He proton spectrum measured using CPS-2 with 1 mm slit for shot 13975. This is a D–$^3$He capsule with 14.5 $\mu$m CH shell. In contrast to the thin-glass-shell capsule implosion of Fig. 2, this shot results in a non-Gaussian, broader than Doppler spectrum. The centroid has an energy down-shift of about 0.8 MeV.

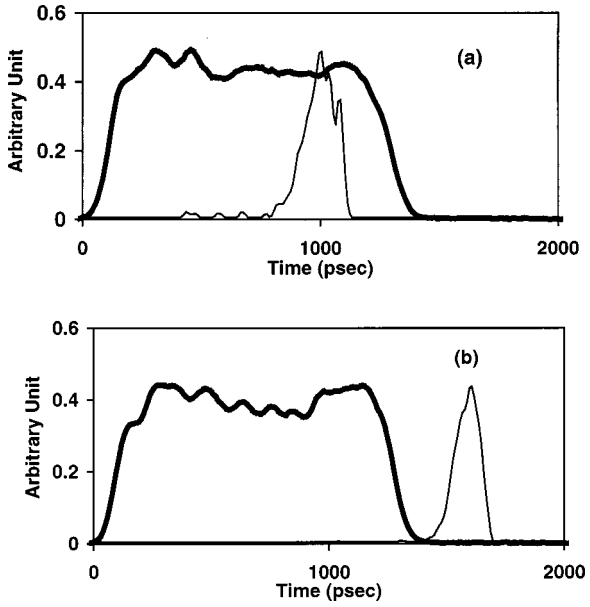


FIG. 4. (a) Neutron temporal measurement (NTD) for shot 13402 (3.3 $\mu$m glass shell). The dark-solid line represents the laser pulse. The bang time occurred during the laser pulse at about 1 ns, and the burn duration was about 150–200 ps. (b) NTD measurement for shot 13410 (3.2 $\mu$m glass + 2.3 $\mu$m HCl + 9.3 $\mu$m CH shell). The bang time occurs at about 1.6 ns, which is a few hundred ps after the laser pulse. By that time the electrostatic fields have largely decayed away (Refs. 7 and 22).

duration (as predicted by LILAC 1-D simulations), or that an extended source exists during the burn, or that nonuniformities exist in the shell. (We believe that energy straggling cannot account for the spectral broadening.)

Returning first to thin-glass-shell capsules (Fig. 2), acceleration or energy up-shift due to capsule charging was observed. Such effects appear to be important whenever the bang time occurs while the laser is on. This will happen for thin-glass-shell capsules driven by 1 ns pulses, but not for thick-plastic-shell capsules driven by 1 ns pulses, nor for thin-glass-shell capsules driven by 400 ps pulses. In both the latter cases the electrostatic field will have largely decayed away.[7,22] In particular the data show that for 400 ps pulses, thin-glass-shell capsule implosions have little energy up-shift.[23] To illustrate these points, Figs. 4(a) and 4(b) depict the neutron temporal detector burn history measurements for both thin-glass- and thick-plastic-shell implosions. These considerations are summarized in Fig. 5 where the one-dimensional (1D) code (LILAC[24]) calculated bang times are plotted vs capsule initial areal densities. Figure 6(a) summarizes the experimental data of energy shifts of the 14.7 MeV proton line for both thin-glass- and thick-plastic-shell capsules driven by 1 ns pulses. Another way of looking at this same phenomenon, in terms of directly measured quantities, is to plot the energy shift vs initial shell areal density [Fig. 6(b)].

## IV. DETERMINATIONS OF SHELL $\rho R$ AND FUEL $T_i$

### A. Shell areal density measurements

In this section we determine the areal densities achieved for thick-plastic-shell capsule implosions. This is done by

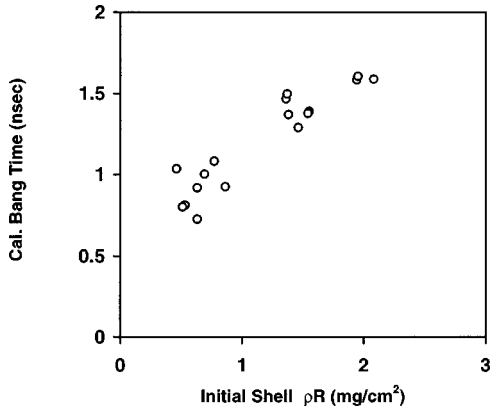


FIG. 5. 1D LILAC predicted bang times are plotted vs capsule initial shell areal densities. (Calculated and experimental bang time measurements are in good agreement.) The laser pulses were about 1 ns square (on top). The larger the initial shell $\rho R$, the later the bang time. Note that because of slight differences in the experimental conditions, such as gas pressure, laser energy, pulse duration, etc., the bang time may be different for shots that have same initial shell $\rho R$.

directly measuring the amount of energy lost by D–$^3$He protons while traversing the fuel and shell (although the shell $\rho R$ dominates the energy loss process[25,26]). To illustrate this situation, Fig. 7 shows a 14.7 MeV proton spectrum for shot 13799. This was a 938 $\mu$m diameter capsule with 18.4 $\mu$m thick CH, filled with 2.8 atm of $D_2$ and 4.9 atm of $^3$He. The target was irradiated with 28.3 kJ of UV light with 2D–SSD (0.2 THz) smoothing and 1 ns square-top pulse. For this implosion, the energy loss is about 1.8 MeV. Utilizing range-energy curves, such as shown in Fig. 8,[25,26] we estimate the fuel and shell areal density to be about $75 \pm 8$ mg/cm$^2$. From the MEDUSA single-hit neutron detector array, an upper limit of the fuel $\rho R$ is determined to be about 13.0 $\pm 3$ mg/cm$^2$. Because the fuel $\rho R$ is small, the shell $\rho R$ can be well estimated by the following formula:

$$\rho R_{\text{shell}} \approx \rho R_{\text{total}} - [(dE/dx)_{\text{fuel}}/(dE/dx)_{\text{shell}}]\rho R_{\text{fuel}}, \quad (1)$$

where $dE/dx$ is the stopping power and $\rho R_{\text{total}}$ is calculated under the assumption that the $T_e$ is that of shell. Consequently, the shell $\rho R$ is estimated to be about 65 $\pm 11$ mg/cm$^2$. Figure 9 summarizes the data of all thick-plastic-shell implosions, for which shell $\rho Rs$ vary between 20–70 mg/cm$^2$.

A comparison of the measured spectrum in Fig. 7 with predictions of the 1D simulation code LILAC illustrates the utility of the CPS data for benchmarking the simulations. Specifically the code prediction for the energy down-shift is ~4.5 MeV, about 2.5 times larger than the experimental measurement. The corresponding fuel and shell $\rho R$ code (experimental) predictions are 34 (13) mg/cm$^2$ and 120 (65) mg/cm$^2$, respectively. Although the code and experimental ion temperatures are quite similar (~4 keV), as can be seen from Fig. 7 the 1D D–$^3$He yield prediction is about a factor of 3 higher than the measurement. The reasons for the various discrepancies are presently under investigation.

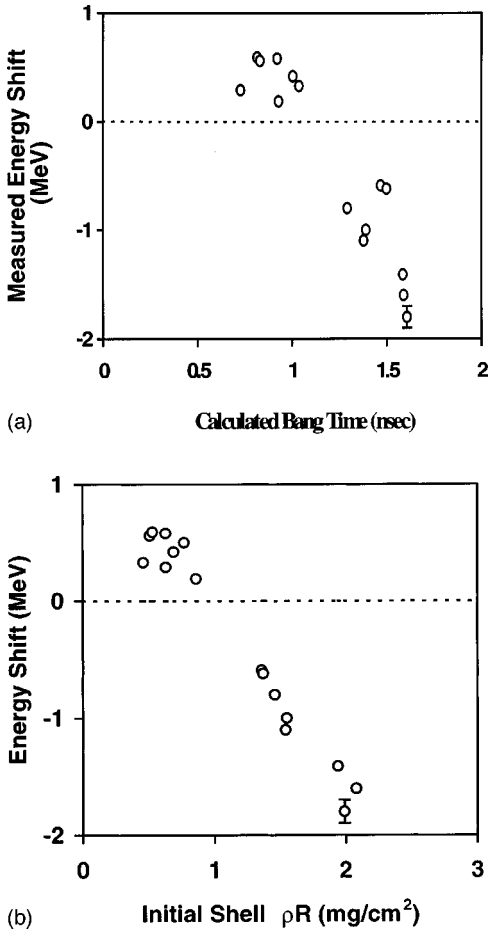


FIG. 6. (a) Measured energy shifts are plotted vs 1D LILAC predicted bang times. For thin-glass-shell capsules, measured D–$^3$He protons were energy up-shifted due to acceleration effects. For thick-plastic-shell capsules, for which acceleration effects are small, the line is down-shifted due to ranging effects. (b) Measured energy shifts of D–$^3$He protons as a function of initial shell $\rho R$. Protons from thin-glass-shell capsules have some energy up-shift because, first, accelerating electric fields can occur while the laser is on and, second, the shell $\rho R$ is not high enough to significantly slow down the protons. Protons from thick-plastic-shell capsules have little if any acceleration (since bang time occurs well after the laser is turned off), but do suffer significant energy loss in traversing the shell. At present, model independent areal densities (Fig. 9) can be determined only for thick-shell capsules.

### B. Ion temperature measurements

In this section we illustrate the utility of the CPS data for ion temperature determination. For thin-glass-shell capsules, multiple charged-fusion products (D–$^3$He and D–D protons, D–$^3$He alphas, and D–D tritons) can be simultaneously obtained. For example, Figs. 10(a) and 10(b) show typical spectra of D–$^3$He and D–D protons, respectively, from a D–$^3$He shot (shot 13 825). Taking the ratio of these two yields for the experimental conditions of equal molar D and $^3$He, and under the assumption of a uniform density and temperature for the fuel, results in a well-defined function of the temperature (Fig. 11 gives the relation between this ratio and $T_i$)

$$Y_{\text{DDn}}/Y_{\text{D}^3\text{Hep}} = 0.5\langle\sigma v\rangle_{\text{DDn}}/\langle\sigma v\rangle_{D^3\text{Hep}}, \quad (2)$$

where $\langle\sigma v\rangle_{\text{DDn}}$ ($\langle\sigma v\rangle_{D^3\text{Hep}}$) is the rate coefficient for D–Dn (D–$^3$He) reaction.

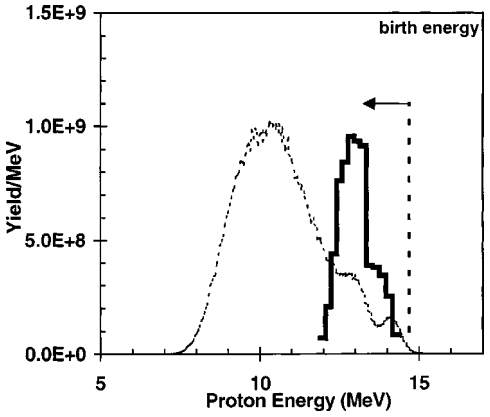


FIG. 7. Measured proton spectrum (dark-solid line) of a thick-plastic-shell capsule (shot 13799, 18.4 $\mu$m CH), measured with CPS-2 (1 mm slit), compared to the birth energy of D–$^3$He protons (14.7 MeV) and to the 1D LILAC simulation (dashed line). The measured down-shift is about 1.8 MeV, which is smaller than LILAC's prediction of ~4.5 MeV.

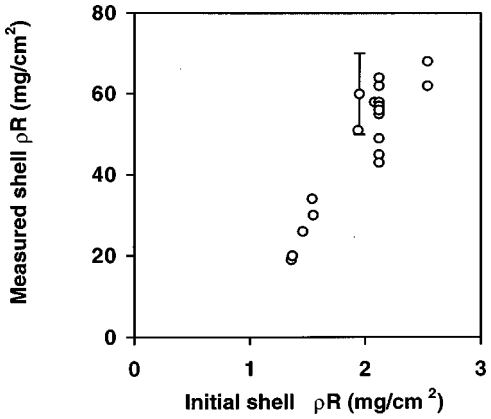


FIG. 9. Measured shell areal densities vs corresponding initial areal densities of thick-plastic-shell capsules. The error bar is largely systematic in nature. Statistical errors are much smaller.

Ion temperatures were determined in this way for a number of shots, and the results are shown in Fig. 12 [where, for thick-plastic-shell capsules, for which the D–D protons are completely ranged out, we utilize the measured D–D neutron yield after correcting for the (small) effect in the D–D branching ratios[27]]. Temperatures between 3 and 15 keV were obtained, and are plotted vs corresponding temperatures measured by the neutron-doppler time-of-flight diagnostic (TOF). The sizes of the errors involved in the two methods are similar, and are about ±10%. As is seen, both methods are in reasonable agreement. Additionally, the effects of non-uniform fuel temperatures and densities upon the ratio method will be the subject of future investigations.

For the case of thin-glass-shell capsules, ion temperatures can be also determined from the measured widths of charged-particle spectra (doppler method). This method is independent of the fusion cross sections and therefore independent of the absolute particle yields. However, this tech-

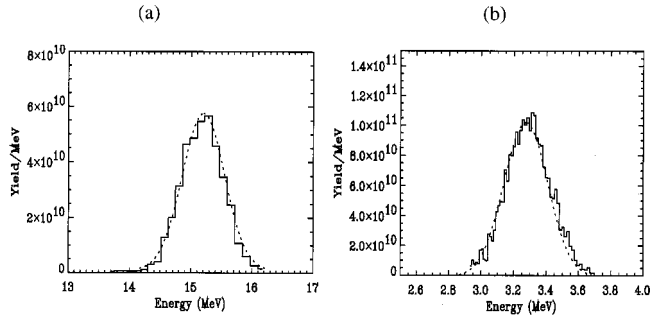


FIG. 10. (a) D–$^3$He proton spectra (from CPS-2) measured from shot 13825 (D–$^3$He capsule with a thin-glass-shell 2.3 $\mu$m, $SiO_2$ shell) for which an energy up-shift of about 0.5 MeV was observed. (b) D–D proton spectra (also from CPS-2) measured for the same shot, with an energy up-shift of about 0.2 MeV (a smaller net up-shift because these lower energy protons have a higher stopping power than the 14.7 MeV protons, consequently more energy is lost traversing the fuel and shell). Ion temperatures were deduced from the yield ratio of these two kinds of protons.

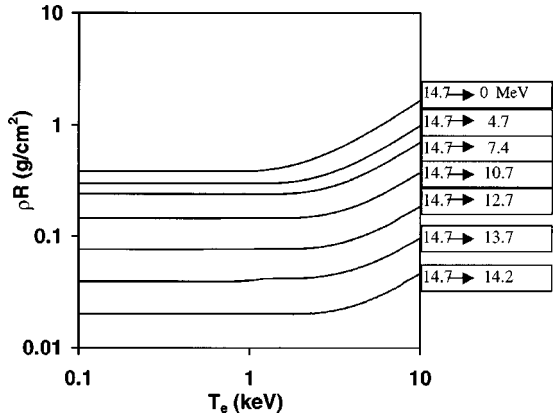


FIG. 8. Range vs electron temperature are calculated for nascent 14.7 MeV protons (Refs. 25 and 26) undergoing different energy losses in a fully ionized CH plasma (ion density assumed was $2\times10^{24}\,\mathrm{cm}^{-3}$, but only a weak density dependence exists for these curves). Of importance to this paper, these curves have a weak temperature dependence for $T_e \leqslant 3$ keV. Shell plasma, which accounts for most of the energy loss of the 14.7 MeV protons, has temperatures well below 3 keV.

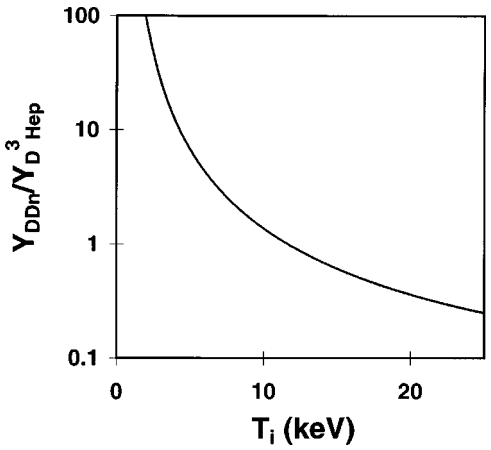


FIG. 11. The ratio of the D–D neutron to the D–$^3$He proton yield, plotted against the ion temperature (assuming a uniform temperature and density for the fuel). Future work will extend this ratio method for the important case of non-uniform temperatures and densities of the fuel.

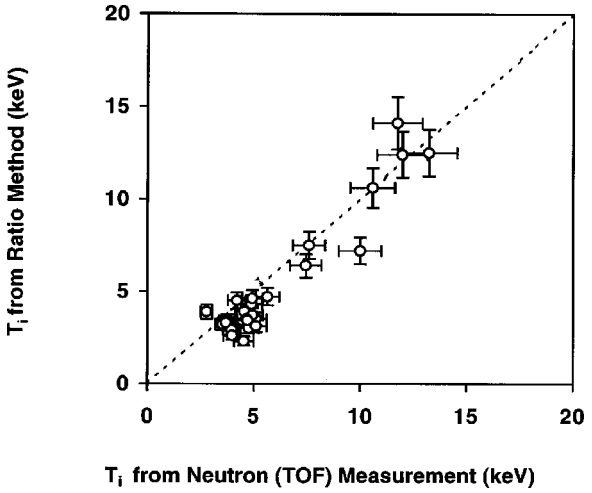


FIG. 12. Ion temperatures measured by using the ratio of D–D neutron yield to D–$^3$He proton yield, plotted against ion temperature determined by neutron time-of-flight spectrometer.

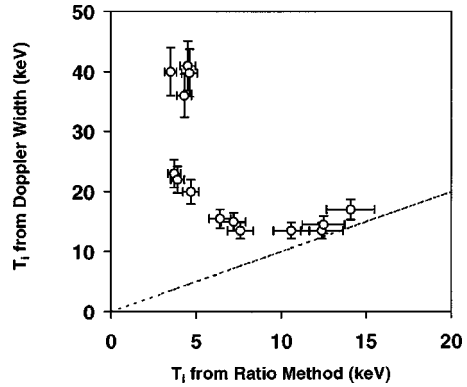


FIG. 14. Comparison of temperatures determined from the doppler width and the ratio method. For thick-plastic-shell implosions ($T_i < 10$ keV), the doppler method significantly overestimates the temperature if the linewidth is treated as solely due to doppler broadening. This overestimate is due to the fact that thick-plastic-shell implosions have linewidths clearly larger than the doppler width (see text).

nique is only valid for thin-glass-shell capsule implosions ($\leqslant 3$ $\mu$m), such as that shown in Fig. 10, since in such instance, the linewidth is dominated by the doppler width. In contrast, thick-plastic-shell capsules have significant broadening due to the evolution of $\rho R$ during the burn; or due to the presence of an extended burn region; or is an indication of nonuniformities in the shell. Fig. 13 illustrates both cases. The agreement and departure of these two methods is illustrated in Fig. 14.

## V. SUMMARY AND CONCLUSIONS

In summary, high-resolution D–$^3$He proton energy spectra have been obtained for the first time, and were utilized to deduce areal densities and ion temperatures of imploded capsules on OMEGA. Shell areal densities between 20 and 70 mg/cm$^2$ and ion temperatures between 3 and 15 keV have been determined for 25 shots. Some departures of the measurements from 1D, zero-mix code (LILAC) were noted. Determination of $T_i$ with the ratio method is found to be useful for both thin-glass- and thick-plastic-shell capsules, and is in reasonable agreement with neutron measurements. In contrast, the doppler method for $T_i$ determination works well only for thin-glass-shell capsules for which the spectra are dominated by the doppler width. For thick-plastic-shell capsule implosions, the linewidths are clearly larger than doppler widths. The reasons for this effect are the subject of future study.

In conclusion, the utility of the experimental results described herein bodes well for the proposed use of 31-MeV teriary protons for determining the areal density (and potential $\rho R$ asymmetries) at the National Ignitioni Facility (NIF). At the NIF we anticipate very large areal densities ($\sim$1g/cm$^2$) that would range out 14.7-MeV protons but not the 31-MeV protons.[28]

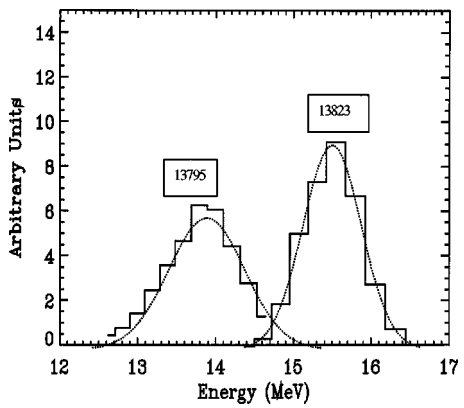


FIG. 13. D–$^3$He proton spectra from two different shots. Shot 13823 is a typical thin-glass-shell (2.2 $\mu$m glass) capsule implosion with an 0.8 MeV energy up-shift due to acceleration. Shot 13975 is a much thicker-plastic-shell capsule (14.6 $\mu$m CH) for which an 0.8 MeV energy down-shift was measured due to the energy loss occurring when protons travel through the fuel and especially the shell. For the thin-glass-shell implosions, the doppler width leads to a $T_i$ that is in reasonable agreement to that determined by ratio method. However, line broadening of a thick-plastic-shell capsule is dominated by non-doppler effects, which, if uncorrected and used to deduce the doppler $T_i$, would give an erroneously high temperature of 36 keV (compared to the correct value about 4 keV).

## ACKNOWLEDGMENTS

For their efforts in implementing numerous aspects of the charged-particle spectrometers, we express our appreciation to the OMEGA engineering group, to the Laser and Experimental Operations team, and to the Target Fabrication crew. We also gratefully acknowledge the continuous support of Prof. R. McCrory, Dr. W. Seka and Mr. S. Loucks of LLE at U. of Rochester, and Prof. M. Porkolab of MIT. This work has been supported in part by LLE (subcontract No. P0410025G) and Lawrence Livermore National Laboratory (subcontract No. B313975), and by the U.S. Department of Energy (DOE) Office of Inertial Confinement Fusion under Cooperative Agreement No. DE-FC03-92SF19460, the University of Rochester, and New York State Energy Research and Development Authority. The support of DOE does not constitute an endorsement by DOE of the views expressed in this work.

[1]J. D. Lindl, R. L. McCrory, and E. M. Campbell, Phys. Today **45**, 32 (1992).
[2]J. D. Lindl, *Inertial Confinement Fusion* (Springer-Verlag, New York, 1998).
[3]T. R. Boehly *et al.*, Opt. Commun. **133**, 496 (1997).
[4]S. Skupsky and S. Kacejar, Appl. Phys. Lett. **52**, 2608 (1981).
[5]S. Kacejar *et al.*, Phys. Rev. Lett. **49**, 463 (1982).
[6]Y. Kitagawa *et al.*, Phys. Rev. Lett. **77**, 3130 (1995).
[7]Y. Gazit *et al.*, Phys. Rev. Lett. **43**, 1943 (1979).
[8]D. G. Hicks *et al.*, Rev. Sci. Instrum. **68**, 589 (1997).
[9]D. G. Hicks, Ph.D. thesis, Massachusetts Institute of Technology, 1999.
[10]R. J. Leeper *et al.*, J. Appl. Phys. **60**, 4059 (1986).
[11]The ability to measure yields up to $10^{16}$ is based upon experimental data of ablator protons (Ref. 23).
[12]Energy resolution is defined as the ability to distinguish between two lines.
[13]S. Skupsky and R. S. Craxton, Phys. Plasmas **6**, 2157 (1999).
[14]M. A. Russotto and R. L. Kremens, Rev. Sci. Instrum. **61**, 3125 (1990).
[15]J. D. Kilkenny *et al.*, Rev. Sci. Instrum. **66**, 288 (1995).
[16]R. J. Leeper *et al.*, Rev. Sci. Instrum. **68**, 868 (1997).
[17]J. P. Knauer, R. L. Kremens, M. A. Russotto, and S. Tudman, Rev. Sci. Instrum. **66**, 926 (1995).
[18]M. D. Cable, S. P. Hatchett, and M. B. Nelson, Rev. Sci. Instrum. **63**, 4823 (1992).
[19]R. A. Lerche, D. W. Phillion, and G. L. Tietbohl, Rev. Sci. Instrum. **66**, 933 (1995).
[20]Random variations in yields, non statistical in nature, about $\pm 25\%$ are typically seen between CPS-1 and CPS-2 (Ref. 9). This variation, the subject of future study, is partly responsible for the vertical ''uncertainty'' in Fig. 12, and the horizontal ''uncertainty'' in Fig. 14.
[21]C. K. Li *et al.* (unpublished).
[22]J. Delettrez *et al.*, Nucl. Fusion **23**, 1135 (1983).
[23]D. G. Hicks *et al.* (unpublished).
[24]E. Goldman, Laboratory for Laser Energetics Report No. 16, Univ. of Rochester, 1973.
[25]C. K. Li and R. D. Petrasso, Phys. Rev. Lett. **70**, 3059 (1993).
[26]C. K. Li and R. D. Petrasso, Phys. Plasmas **2**, 2460 (1995).
[27]D. L. Book, *NRL Plasma Formulary* (U.S. Naval Research Laboratory, Washington, DC, 1990).
[28]R. D. Petrasso *et al.*, Phys. Rev. Lett. **77**, 2718 (1996).